

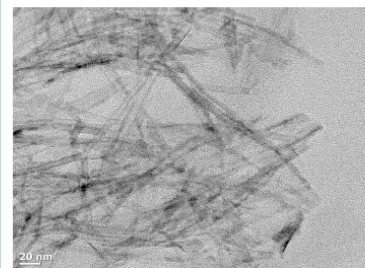
Characterization of Hydrothermally Prepared Titanate Nanotube Powders by Ambient and In Situ Raman Spectroscopy

Sun-Jae Kim,[†] Yeong-Ung Yun,[†] Hyo-Jin Oh,[†] Sung Ho Hong,[‡] Charles A. Roberts,[§] Kamalakanta Routray,[§] and Israel E. Wachs^{*,§}

[†]Nano Materials Laboratory, Faculty/Institute of Nanotechnology & Advanced Materials Engineering, Sejong University, 98 Gunja-dong, Gwangjin-gu, Seoul 143-747, Korea, [‡]Environment Project Department, Strategic Project Division, Korea Power Engineering Company Inc., 360-9 Mabuk-dong, Giheung-gu, Yongin-si, Gyeonggi-do 446-713, Korea, and [§]*Operando* Molecular Spectroscopy & Catalysis Laboratory, Department of Chemical Engineering, Lehigh University, Bethlehem, Pennsylvania 18015, USA

ABSTRACT This letter reports on the successful synthesis of hydrogen titanate nanotubes (H-Ti-NT) and TiO₂ (anatase) nanotubes and their thermal solid-state transformational chemistry and clarifies some of the confusion surrounding their literature Raman vibrational assignments. Hydrothermally prepared titanate nanotube powders with negligible (< 0.1 wt % Na, H-Ti-NT) and high (~7.0 wt % Na, Na/H-Ti-NT) Na content, that underwent freeze-drying and thermal treatments, were prepared and characterized with ambient and in situ Raman spectroscopy. The H-Ti-NT phase gives rise to Raman bands at ~195, 285, 458, ~700, 830, and 926 cm⁻¹. The Raman bands above 650 cm⁻¹ were found to be sensitive to the presence of moisture, which indicates that they are related to surface vibrational modes. The titanate nanotube Raman band at ~926 cm⁻¹ was shown not to be related to a Na-O-Ti vibration, which was previously assigned in the literature, since its intensity does not vary with Na content, which varied by a factor of > 70. The nanotubular H-Ti-NT phase was found to be thermally stabilized, < 700 °C, by Na that had been entrapped during synthesis. The Na-free H-Ti-NT phase, however, transformed to TiO₂ (anatase) nanotubes upon heating above 200 °C and was stable up to 700 °C.

SECTION Nanoparticles and Nanostructures



Hydrothermally prepared titanate nanotube (Ti-NT) powders have excellent potential as heterogeneous catalysts,¹⁻⁵ hydrogen storage materials,^{6,7} and secondary batteries⁸⁻¹⁰ because of their nanoscale tubular shape (outer diameter ~ 1 nm) and large internal open structure (internal diameter ~ 0.6–0.8 nm). These characteristics are responsible for the high surface area and large pore volume of titanate nanotubes. It has been reported that these titanate nanotubes are easily converted into nanospherical or rod-like particles at temperatures above 500 °C in air.¹¹ If the nanotubular-shaped titanate is thermally converted to high-surface-area titania without changing its morphology, it potentially can have applications as a photo- or thermal catalyst and as a catalytic support material. Nanotubular titania has especially strong merit as a humidity sensor or catalytic support material. The large surface area of such a nanotubular titanate can support and disperse relatively large amounts of active catalytic components such as Pt, MoO₃, WO₃, V₂O₅, and so forth. Furthermore, the large external and internal surfaces with planar sites of the nanotubular titanate would facilitate uniform reaction over its surface.^{2,4,12,13}

The ideal oxide support material for a stable gas sensor or heterogeneous catalyst should not show any changes in physical properties such as shape, crystalline structure, and surface area during thermal treatments and under realistic operating environments. The nanotubular titanate phase changes during thermal treatments, however, have not previously been clearly established or tracked. This lack of uniform conclusions is a consequence of differing reports about the TiO₂ or titanate phase in the as-prepared or dried powders and about the remaining content of Na in the powder, which differed among the limited literature reports.^{1,5,14-16} In order to address these synthesis variables on the resulting nanotubular titanate structures, the present study employs Raman spectroscopy to investigate the crystalline phases of Ti-NT powders prepared by hydrothermal and freeze-drying methods with negligible and high Na contents. The freeze-drying method was employed to exclude any thermal effects on the

Received Date: September 22, 2009

Accepted Date: November 3, 2009

Published on Web Date: November 10, 2009

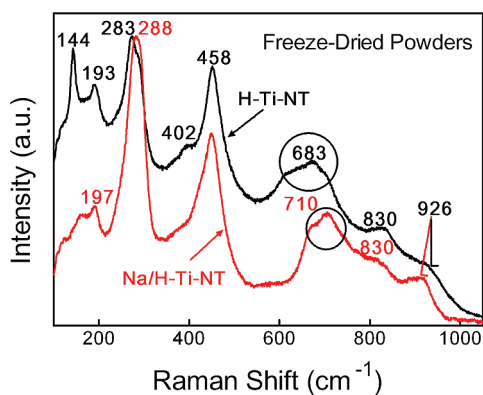


Figure 1. Raman spectra of the as-prepared titanate powders with negligible Na content (H-Ti-NT) and with 7.02 atom % Na content (Na/H-Ti-NT) under ambient conditions.

crystallinity that may be caused by the rapid removal of H₂O or H⁺ from the powder and to also study the effect of water on the crystallinity of the Ti-NT powder. The elemental Na content in the as-prepared powders was controlled by varying the number of water-washing treatments and employing an additional ion exchange technique.

Raman spectroscopy is an ideal characterization method for oxide powders since it can provide both bulk and surface molecular structural information under various environmental conditions.¹⁷ Furthermore, Raman spectroscopy can also readily discriminate between the different crystalline morphologies of TiO₂ (anatase, rutile, brookite, B, and Ti-NT)^{18–22} and tungsten oxide phases (bulk WO₃ and surface WO_x species)^{23–25} that are many times added as promoters to TiO₂ catalysts.

The Raman spectra of the as-prepared, freeze-dried H-Ti-NT and Na/H-Ti-NT ambient powders with long nanotubular shapes, which were previously reported,^{5,11} are presented in Figure 1.

The Raman spectrum of the Na/H-Ti-NT powder has the bands characteristic of the titanate phase (197, 288, 458, 710, 830, and 926 cm⁻¹).^{19–22} The crystalline structure of Na/H-Ti-NT, however, is still uncertain due to the coexistence of mixed orthorhombic and monoclinic crystalline phases. The Raman spectrum of the low Na H-Ti-NT powder exhibits somewhat broader Raman bands of the titanate phase that are slightly blue-shifted (193, 283, 458, 683, 830, and 926 cm⁻¹) and contains additional bands at 144 and 402 cm⁻¹ from a trace amount of TiO₂ (anatase).²⁶ The titanate Raman spectrum was compared with reference Raman spectra (Figure S1, Supporting Information) of different TiO₂ phases (anatase, rutile, brookite, and B), and anatase was the only additional phase found to be present in the titanate samples. The relative intensity of the small TiO₂ (anatase) Raman band was found to increase as the Na content was decreased during the intermediate ion exchange stages in the preparation of H-Ti-NT (not shown for brevity), which is in agreement with similar observations previously reported by Kasuga et al.^{27,28}

The relative Raman cross sections of the Ti-NT and TiO₂ (anatase) phases were semiquantitatively determined from a series of physical mixtures of the two crystalline phases (see Supporting Information Figures S2 and S3), and a rough

estimate of the amount of the TiO₂ (anatase) phase was made. It is estimated that ~1.0 wt % TiO₂ (anatase) is present in the H-Ti-NT powder. Kasuga et al. reported preparation of TiO₂ (anatase) nanotube powder from continuous washing and ion exchange using aqueous HNO₃ solution. The SEM and TEM images of their final powder contained short or disrupted nanotube shapes, and the corresponding Raman spectrum was dominated by vibrations from the TiO₂ (anatase) phase with weak titanate bands at ~280 and 700 cm⁻¹.^{27,28} From analysis of the Raman spectra of the Ti-NT and TiO₂ (anatase) physical mixtures shown in Figures S2 and S3 (Supporting Information), it is estimated that their powders contained ~40 wt % TiO₂ (anatase). It was also observed in the present study that after extensive washing and ion exchange treatments that the original Ti-NT micrometer long nanotubes changed into very short tubes with strong TiO₂ (anatase) Raman bands. In the present study, the nanotubular H-Ti-NT powder was successfully synthesized with only a trace of TiO₂ (anatase), ~1.0 wt %, and negligible Na content, <0.1 atom %. Thus, it can be inferred that with extensive washing, a significant portion of the titanate phase transforms into the TiO₂ (anatase) phase with concomitant destruction of the nanotubular shape and almost complete removal of Na.

The Raman spectrum of the ambient H-Ti-NT powder has a somewhat broader band in the 600–720 cm⁻¹ range (circled area in Figure 1) than the Raman spectrum of the ambient Na/H-Ti-NT powder. Thermogravimetric analysis revealed that the H-Ti-NT powder possessed 23% more water than the Na/H-Ti-NT powder. The 23% water difference in the two samples can be attributed to the more porous structure of the H-Ti-NT powder (BET, ~350 m²/g) compared to the Na/H-Ti-NT powder (BET, ~300 m²/g)¹¹ since almost the same weight loss pattern with increasing temperature was obtained for both powders. Therefore, the greater broadening of the Raman bands in H-Ti-NT may be related to the greater water content in this nanotubular titanate powder.

Additional insight into the effect of moisture upon broadening of the Raman bands of the H-Ti-NT powder around 700 cm⁻¹ was obtained by comparing multiple freeze-drying cycles and drying methods, as indicated in Figure 2. The numbers contained in Figure 2a indicate the number of freeze-drying cycles to decrease the amount of H₂O in the powder. For example, #5 means the freeze-drying cycle was carried out 5 times and for 24 h each time without raising the temperature. Referencing to the total moisture weight loss after calcination at 1000 °C, the total H₂O content of the H-Ti-NT powder decreased from 44 to 12 wt % with these multiple freeze-drying cycles. The H₂O content dropped from 44 to 10 and 8.6 wt % for convection drying and vacuum drying at 105 °C, respectively. With decreasing H₂O content in the powder, the broad Raman band at around 700 cm⁻¹ becomes narrower with freeze-drying (Figure 2a) and further sharpens with the more efficient drying at 105 °C (Figure 2b). The observed sharpening of the bands with removal of water is in agreement with previous studies exhibiting the sharpening of Raman bands upon sample dehydration.²⁹

The other major Raman bands below 600 cm⁻¹, however, were almost unchanged, regardless of further sample drying treatment. Thus, the H-Ti-NT titanate band at ~700 cm⁻¹ is

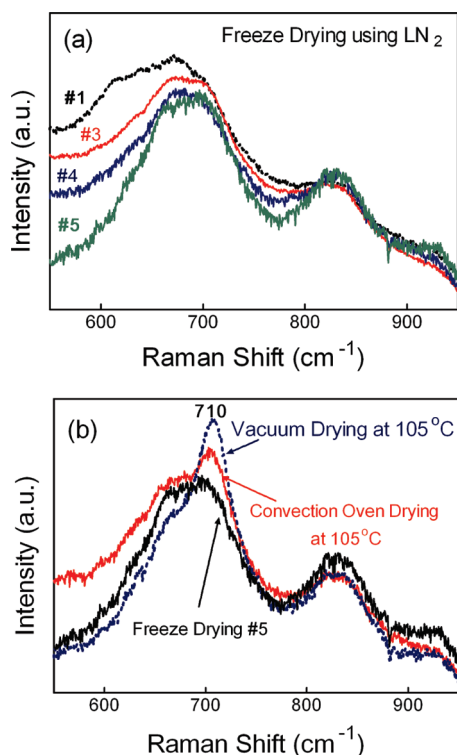


Figure 2. Raman spectra of the titanate powders with negligible Na content (H-Ti-NT) freeze-dried multiple times (a) and of the powders with various drying methods (b) under ambient conditions.

sensitive to moisture and sharpens and shifts from ~ 683 to ~ 710 cm^{-1} upon dehydration and suggests that this band as well as the weaker bands at ~ 830 and ~ 926 cm^{-1} may be related to surface vibrational modes.

The Raman spectra of ambient Na/H-Ti-NT and H-Ti-NT titanates in Figures 1 and 2 also exhibit a small band at 926 cm^{-1} that was previously assigned to bridging Na-O-Ti bonds formed by surface Na on the titanate particles.^{19,30-33} Note that this broad Raman band also sharpens upon dehydration, as shown in Figure 2a and b. The comparable intensity of this Raman band for the Na/H-Ti-NT and H-Ti-NT titanates, with the former containing > 70 times more Na and the latter having negligible amounts of Na, strongly suggests that this band is not related to the bridging Na-O-Ti vibrations. The ~ 926 cm^{-1} titanate Raman band may be related to an overtone of the 453 – 458 cm^{-1} band.

Another way to probe the presence of surface Na in these titanates is to examine their effect on the vibrations of the dehydrated supported WO_3 /titanates since the surface W=O vibration is extremely sensitive to the presence of surface sites with alkali properties.^{34,35} Surface $\text{O}=\text{WO}_4$ species vibrate at ~ 1010 – 1020 cm^{-1} , and the presence of surface alkali shifts the W=O band to ~ 900 – 950 cm^{-1} under dehydrated conditions.^{34,35} The in situ Raman spectra of the supported $\sim 12\%$ WO_3 /titanate powders were taken at 700 $^\circ\text{C}$, as shown in Figure S4 (Supporting Information), and neither sample possesses a strong Raman band at ~ 805 cm^{-1} characteristic of crystalline WO_3 .²⁰ The supported WO_3 /Na/H-Ti-NT sample

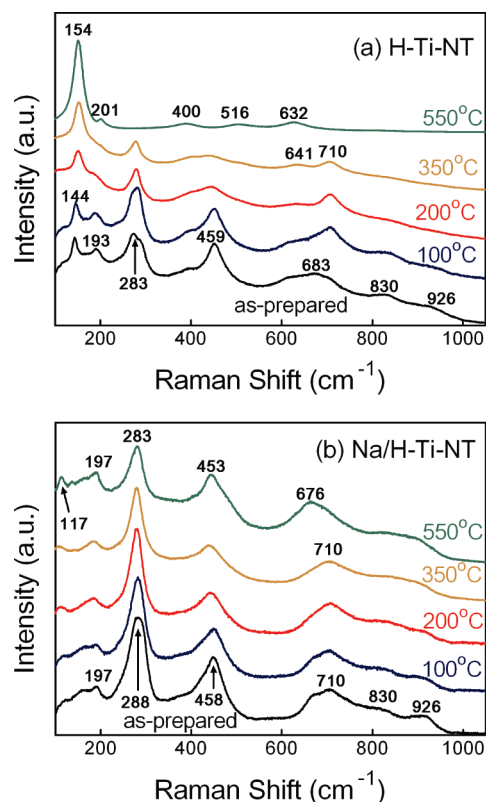


Figure 3. In situ Raman spectra of the titanate powders (a) with negligible Na content (H-Ti-NT) and (b) with 7.02 atom % Na content (Na/H-Ti-NT) taken at temperatures of 100 to 550 $^\circ\text{C}$ with a flowing 10% O_2/Ar (30 sccm).

exhibits W=O Raman bands at 905 and 922 cm^{-1} , reflecting the presence of surface Na complexing with the surface WO_x species. The supported WO_3 /H-Ti-NT sample, however, contains the W=O vibration at 1009 cm^{-1} , consistent with the almost complete absence of surface Na in this nanotubular titanate powder.^{34,36,37} Furthermore, a sample with ~ 0.10 – 0.15 atom % Na resulted in a shift of the W=O Raman band to ~ 950 cm^{-1} (not shown for brevity). Thus, the H-Ti-NT titanate powder prepared in this investigation is almost completely free of surface Na.

In situ Raman measurements were also conducted between 100 and 550 $^\circ\text{C}$ in an oxidizing atmosphere to monitor the thermal behavior of the H-Ti-NT and Na/H-Ti-NT powders, and the corresponding spectra are presented in Figure 3a and b, respectively. Up to 350 $^\circ\text{C}$ for H-Ti-NT, the initial broad band at 600 – 720 cm^{-1} sharpens and splits into two bands corresponding to the titanate phase at 710 cm^{-1} and to the anatase phase at 641 cm^{-1} .

The sharpening of this Raman band upon desorption of moisture further suggests that the H-Ti-NT Raman band is related to a surface vibrational mode. Up to 550 $^\circ\text{C}$, the H-Ti-NT phase completely transforms to the anatase phase (632 cm^{-1}). In contrast, the Raman bands of the Na/H-Ti-NT powder contain almost the same intensity up to 200 $^\circ\text{C}$, which slightly decreases at higher temperatures due to thermal broadening, and also become blue-shifted due to temperature effects. However, the Na/H-Ti-NT phase does not

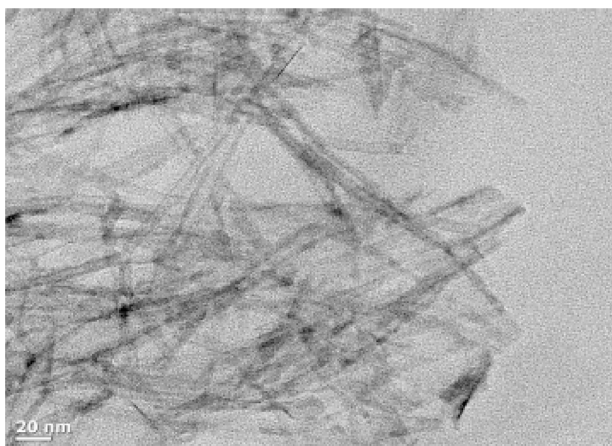


Figure 4. TEM photo for the H-Ti-NT powder after heat treatment at 400 °C for 30 min in air.

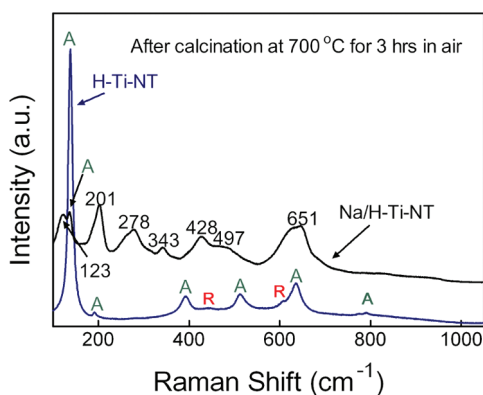


Figure 5. Raman spectra of the titanate powders with negligible Na content (H-Ti-NT) and with 7.02 atom % Na content (Na/H-Ti-NT) under ambient conditions after calcining at 700 °C for 3 h in air (A: anatase phase, R: rutile phase).

transform to TiO₂ (anatase) below 550 °C, and a new minor band appears at ~117 cm⁻¹ that is reminiscent of Na₂Ti₃O₇.³³ These comparative thermal studies clearly demonstrate that Na stabilizes the H-Ti-NT titanate phase at elevated temperatures and that in the absence of Na, the H-Ti-NT phase transforms to TiO₂ (anatase).

Transmission electron microscopy (TEM, JEOL-2010) was employed to image the titanate particle shapes present in the sample. The TEM image of the anatase Ti-NT powder obtained after calcination at 400 °C for 30 min is shown in Figure 4.

The image shows that the powder still consists of a long nanotube shape that is unaffected by calcination at 400 °C. The image was used to estimate the inner and outer diameters of the nanotubes at ~1 and ~0.75 nm, respectively, with an estimated error of 10–20%.

The Raman spectra of the ambient H-Ti-NT and Na/H-Ti-NT titanate powders after calcination at 700 °C for 3 h in air are presented in Figure 5.

These spectra show sharp Raman bands at 138, 191, 393, 513, 638, and 796 cm⁻¹ corresponding to the TiO₂ (anatase) phase crystals of micrometer-sized particles and only traces of the TiO₂ (rutile) phase at 450 and 614 cm⁻¹ that are marked A

and R, respectively, in Figure 4. The complete absence of TiO₂ (rutile) during calcination of H-Ti-NT below 700 °C for 3 h indicates that the TiO₂ (anatase) nanotubes are thermally stable below 700 °C. The Raman spectrum of the Na/H-Ti-NT powder after calcination at 700 °C contains bands that are characteristic of multiple titanate phases. Qamar et al. previously reported that the titanate nanotube particles with almost the same Na content as that of Na/H-Ti-NT in the present study changed into nanospherical- or nanorod-shaped particles at high temperatures above 500 °C in air with corresponding Raman bands of TiO₂ (anatase), Na₂Ti₃O₇, Na₂Ti₆O₁₃, and so forth.¹¹ Comparison of the current Raman spectrum of Na/H-Ti-NT calcined to 700 °C with those reported by Horvth et al.,³⁵ Papp et al.,³⁸ and Mao et al.³⁹ suggests that the Raman bands of the calcined Na/H-Ti-NT powder in Figure 5 correspond to Na₂Ti₃O₇ and Na₂Ti₆O₁₃, but the bands are slightly shifted. Thus, calcination of Na/H-Ti-NT at 700 °C results in a mixture of H-Ti-NT, Na₂Ti₃O₇, Na₂Ti₆O₁₃, and a small amount of TiO₂ (anatase), and calcination of H-Ti-NT with negligible Na at the same temperature yields the TiO₂ (anatase) phase with a trace of TiO₂ (rutile).

Hydrothermally prepared titanate nanotube powders with negligible and high Na content were prepared and characterized with Raman spectroscopy as a function of synthesis procedures and thermal treatments. The as-prepared nanotube powders primarily consist of the H-Ti-NT phase (Raman bands at ~195, 285, 458, ~700, 830, and 926 cm⁻¹). Moisture was found to broaden the Raman bands at ~700, 830, and 926 cm⁻¹, suggesting that they are related to surface vibrational modes. The titanate Raman band at 926 cm⁻¹, which was previously assigned in the literature as originating from Na-O-Ti vibrations, is present in both titanate samples, where the Na content varies by a factor of > 70, revealing that this band is not related to a Na-O-Ti vibration. The Na-containing titanate powder is thermally stabilized by Na and decomposes at 700 °C to multiple titania phases (H-Ti-NT, Na₂Ti₃O₇, Na₂Ti₆O₁₃, and a small amount of TiO₂ (anatase)). The H-Ti-NT phase with negligible Na, however, readily transforms to TiO₂ (anatase) nanotubes upon calcination between 200 and 700 °C. Thus, this letter reports on the successful synthesis of Na/H-Ti-NT and H-Ti-NT nanotubes and clarifies some of their Raman assignments and their thermal solid-state chemistry.

Experimental Section

Commercial P-25 powder (Degussa) was used as the source of TiO₂ for preparation of the Ti-NT powder. A precursor solution of P-25 and 10 M NaOH in a 304 stainless steel autoclave was subjected to heat treatment at 130 °C for 24 h. The autoclave was lined with a Ni plate to protect it from corrosion by the strongly basic NaOH solution. After hydrothermal synthesis, the precipitated titanates were washed with distilled water (pH = 7.0) several times. At this point, a small amount of sample was collected and termed as Na/H-Ti-NT. The Na content of this sample was found to be 7.02 atom %. The remaining sample was treated with a 0.1 N HCl solution (pH = 1.0) and constantly stirred for 24 h at room

temperature. It was further washed with distilled water at pH = 7.0 to reduce the Na content. The obtained sample was termed H-Ti-NT and found to contain less than 0.1 atom % Na. The elemental Na contents were measured with EDS (energy dispersive spectroscopy) attached to a scanning electron microscope (SEM S-4700, Hitachi Co.). During the 24 h stirring procedure, fresh aqueous HCl solution was introduced every 4 h to ensure rapid ion exchange of the Na ions in the titanate with H ions. The as-prepared Ti-NT powders were obtained after complete washing by freeze-drying at $-57\text{ }^{\circ}\text{C}$ for 24 h in a liquid nitrogen solution. In addition, thermogravimetry analysis (TGA) experiments (STA-1500, Sinco Co.) were conducted to measure the H_2O content of the dried Ti-NT samples.

The Raman studies were performed with a Horiba-Jobin Yvon LabRam-IR high-resolution instrument equipped with a visible light laser source (YAG double diode pumped laser, Coherent 315 m, 20 mW). The Raman spectrometer was equipped with a confocal microscope (Olympus BX-30), notch filter (532 nm), $50\times$ objective, and a single-stage monochromator with 900 grooves/mm grating. The Raman spectral resolution was better than 2 cm^{-1} . The laser power was kept below 0.5 mW at the sample so as to minimize any laser-induced alterations of the sample. The scattered light from the sample was passed through the monochromator grating and collected with a visible sensitive LN_2 -cooled CCD detector (Horiba-Jobin Yvon CCD-3000 V). The LabSpec 5 software was used to operate the experimental setup and collect the Raman spectra. The ambient Raman spectra were collected by putting the samples on a glass slide under ambient conditions. The in situ Raman spectra were collected in an environmental reaction cell (Linkam T 1500). During the in situ Raman analysis, a heating rate with $60\text{ }^{\circ}\text{C}/\text{min}$ was maintained, and 10% O_2/Ar was flown through the cell at 30 sccm. The Raman spectra were collected after maintaining 10 min at the desired temperature during the temperature ramping experiments. Transmission electron microscopy (TEM, JEOL-2010) was employed to image the titanate particle shapes present in the sample.

SUPPORTING INFORMATION AVAILABLE Figures S1, S2, S3, and S4 referenced in the text with further descriptions. This material is available free of charge via the Internet at <http://pubs.acs.org>.

AUTHOR INFORMATION

Corresponding Author:

*To whom correspondence should be addressed. E-mail: iew0@lehigh.edu. Phone: (610)758-5149. Fax: (610)758-6555.

ACKNOWLEDGMENT This research was financially supported by the DeNOx catalysis development program of the Electric Power Industry Research & Development Project as well as by the Seoul Research & Business Development Project (NT070123). The Lehigh researchers gratefully acknowledge the support by the Department of Energy-Basic Energy Sciences Grant DE-FG02-93ERG14350.

REFERENCES

- (1) Kasuga, T. Formation of Titanium Oxide Nanotubes Using Chemical Treatments and Their Characteristic Properties. *Thin Solid Films* **2005**, *496*, 141–145.
- (2) Cortes-Jacome, M. A.; Angeles-Chaves, C.; Morales, M.; Lopez-Salinas, E.; Toledo-Antonio, J. A. Evolution of Titania Nanotubes-Supported WO_x Species by in Situ Thermo-Raman Spectroscopy, X-Ray Diffraction and High Resolution Transmission Electron Microscopy. *J. Solid State Chem.* **2007**, *180*, 2682–2689.
- (3) Cortes-Jacome, M. A.; Ferrat-Torres, G.; Ortiz, L. F. F.; Angeles-Chávez, C.; López-Salinas, E.; Escobar, J.; Mosqueira, M. L.; Toledo-Antonio, J. A. In Situ Thermo-Raman Study of Titanium Oxide Nanotubes. *Catal. Today* **2007**, *126*, 248–255.
- (4) Yu, K.-P.; Yu, W.-Y.; Kuo, M.-C.; Liou, Y.-C.; Chien, S.-H. Pt/Titania-Nanotube: A Potential Catalyst for CO_2 Adsorption and Hydrogenation. *Appl. Catal., B* **2008**, *84*, 112–118.
- (5) Qamar, M.; Yoon, C. R.; Oh, H. J.; Lee, N. H.; Park, K.; Kim, D. H.; Lee, K. S.; Lee, W. J.; Kim, S. J. Preparation and Photocatalytic Activity of Nanotubes Obtained from Titanium Dioxide. *Catal. Today* **2008**, *151*, 5–14.
- (6) Lim, S. H.; Luo, J.; Zhong, Z.; Ji, W.; Lin, J. Room-Temperature Hydrogen Uptake by TiO_2 Nanotubes. *Inorg. Chem.* **2005**, *44*, 4124–4126.
- (7) Jung, Y. H.; Kim, D. H.; Kim, S. J.; Lee, K. S. Synthesis and Characterization of Titanate Nanotube for Hydrogen Storage Using Hydrothermal Method with Various Alkaline Treatment. *J. Nanosci. Nanotechnol.* **2008**, *8*, 5094–5097.
- (8) Zhang, H.; Gao, X. P.; Li, G. R.; Yan, T. Y.; Zhu, H. Y. Electrochemical Lithium Storage of Sodium Titanate Nanotubes and Nanorods. *Electrochim. Acta* **2008**, *53*, 7061–7068.
- (9) Kim, D. H.; Lee, K. S.; Yoon, J. H.; Jang, J. S.; Choi, D.-K.; Sun, Y.-K.; Kim, S.-J.; Lee, K. S. Synthesis and Electrochemical Properties of Ni Doped Titanate Nanotubes for Lithium Ion Storage. *Appl. Surf. Sci.* **2008**, *254*, 7718–7722.
- (10) Zhao, Z. W.; Guo, Z. P.; Wexler, D.; Ma, Z. F.; Liu, H. K. Titania Nanotube Supported Tin Anodes for Lithium Intercalation. *Electrochem. Commun.* **2007**, *9*, 697.
- (11) Qamar, M.; Yoon, C. R.; Oh, H. J.; Kim, D. H.; Jho, J. H.; Lee, K. S.; Lee, W. J.; Lee, H. G.; Kim, S. J. Effect of Post Treatments on the Structure and Thermal Stability of Titanate Nanotubes. *Nanotechnology* **2006**, *17*, 5922–5929.
- (12) Liu, J.; Fu, Y.; Sun, Q.; Shen, J. TiO_2 Nanotubes Supported V_2O_5 for the Selective Oxidation of Methanol to Dimethoxymethane. *Microporous Mesoporous Mater.* **2008**, *116*, 614–621.
- (13) Escobar, J.; Toledo-Antonio, J. A.; Cortes-Jacome, M. A.; Mosqueira, M. L.; Perez, V.; Ferrat, G.; Lopez-Salinas, E.; Torres-Garcia Highly Active Sulfided CoMo Catalyst on Nano-Structured TiO_2 . *Catal. Today* **2005**, *106*, 222–226.
- (14) Bavykin, D. V.; Cressey, B. A.; Light, M. E.; Walsh, F. C. An Aqueous, Alkaline Route to Titanate Nanotubes under Atmospheric Pressure Conditions. *Nanotechnology* **2008**, *19*, 275604.
- (15) Peng, H. R.; Lia, G. C.; Zhang, Z. K. Synthesis of Bundle-Like Structure of Titania Nanotubes. *Mater. Lett.* **2005**, *59*, 1142–1145.
- (16) Nian, J.-N.; Teng, H. Hydrothermal Synthesis of Single-Crystalline Anatase TiO_2 Nanorods with Nanotubes as the Precursor. *J. Phys. Chem. B* **2006**, *110*, 4193–4198.
- (17) Banares, M. A.; Wachs, I. E. Molecular Structures of Supported Metal Oxide Catalysts Under Different Environments. *J. Raman Spectrosc.* **2002**, *33*, 359–380.

- (18) Deo, G.; Wachs, I. E. Predicting Molecular Structures of Surface Metal Oxide Species on Oxide Supports under Ambient Conditions. *J. Phys. Chem.* **1991**, *95*, 5889–5895.
- (19) Wachs, I. E.; Kim, T.; Ross, E. I. Catalysis Science of the Solid Acidity of Model Supported Tungsten Oxide Catalysts. *Catal. Today* **2006**, *116*, 162–168.
- (20) Kim, T.; Burrows, A.; Kiely, C. J.; Wachs, I. E. Molecular/Electronic Structure–surface Acidity Relationships of Model-Supported Tungsten Oxide Catalysts. *J. Catal.* **2007**, *246*, 370–381.
- (21) Ross-Medgaarden, E. I.; Knowles, W. V.; Kim, T.; Wong, M. S.; Zhou, W.; Kiely, J.; Wachs, I. E. New Insights into the Nature of the Acidic Catalytic Active Sites Present in ZrO₂-Supported Tungsten Oxide Catalysts. *J. Catal.* **2008**, *256*, 108–125.
- (22) Bavykin, D. V.; Friedrich, J. M.; Walsh, F. C. Protonated Titanates and TiO₂ Nanostructured Materials: Synthesis, Properties, and Applications. *Adv. Mater.* **2006**, *18*, 2807–2824.
- (23) Qian, L.; Du, Z. L.; Yang, S. Y.; Jin, Z. S. Raman Study of Titania Nanotube by Soft Chemical Process. *J. Mol. Struct.* **2005**, *749*, 103.
- (24) Yao, B. D.; C., Y. F.; Zhang, X. Y.; Zhang, W. F.; Yang, Z. Y.; Wang, N. Formation Mechanism of TiO₂ Nanotubes. *Appl. Phys. Lett.* **2003**, *82*, 281–283.
- (25) Hodos, M.; Horvath, E.; Haspel, H.; Kukovec, A.; Konya, Z.; Kiricsi, I. Photosensitization of Ion-Exchangeable Titanate Nanotubes by CdS Nanoparticles. *Chem. Phys. Lett.* **2004**, *399*, 512–515.
- (26) Deo, G.; Turek, A. M.; Wachs, I. E.; Machej, T.; Haber, J.; Das, N.; Eckert, H. Physical and Chemical Characterization of Surface Vanadium Oxide Supported on Titania: Influence of the Titania Phase (Anatase, Rutile, Brookite and B). *Appl. Catal., A* **1992**, *91*.
- (27) Kasuga, T.; Hiramatsu, M.; Hoson, A.; Sekino, T.; Niihara, K. Titania Nanotubes Prepared by Chemical Processing. *Adv. Mater.* **1999**, *11*, 1307–1311.
- (28) Kasuga, T.; Hiramatsu, M.; Hoson, A.; Sekino, T.; Niihara, K. Formation of Titanium Oxide Nanotube. *Langmuir* **1998**, *14*, 3160–3163.
- (29) Jehng, J. M.; Deo, G.; Weckhuysen, B. M.; Wachs, I. E. Effect of Water Vapor on the Molecular Structures of Supported Vanadium Oxide Catalysts at Elevated Temperatures. *J. Mol. Catal.* **1996**, *110*, 41–54.
- (30) Bavykin, D. V.; Friedrich, J. M.; Lapkin, A. A.; Walsh, F. C. Stability of Aqueous Suspensions of Titanate Nanotubes. *Chem. Mater.* **2006**, *18*, 1124–1129.
- (31) Kolen'ko, Y. V.; Kovnir, K. A.; Gavrilo, A. I.; Garshev, A. V.; Frantti, J.; Lebdev, O. I.; Churagulov, B. R.; Tendeloo, O. G. V.; Yoshimura, M. Hydrothermal Synthesis and Characterization of Nanorods of Various Titanates and Titanium Dioxide. *J. Phys. Chem. B* **2006**, *110*, 4030–4038.
- (32) Riss, A.; Berger, T.; Grothe, H.; Bernardi, J.; Diwald, O.; Knozinger, E. Chemical Control of Photoexcited States in Titanate Nanostructures. *Nano Lett.* **2007**, *7*, 433–438.
- (33) Horvath, E.; Kukovec, A.; Konya, Z.; Kiricsi, I. Hydrothermal Conversion of Self-Assembled Titanate Nanotubes into Nanowires in a Revolving Autoclave. *Chem. Mater.* **2007**, *19*, 927–931.
- (34) Ostromecki, M. M.; Burcham, L. J.; Wachs, I. E.; Ramani, N.; Ekerdt, J. G. The Influence of Metal Oxide Additives on the Molecular Structures of Surface Tungsten Oxide Species on Alumina: I. Ambient Conditions. *J. Mol. Catal. A: Chem.* **1998**, *132*, 43–57.
- (35) Ostromecki, M. M.; Burcham, L. J.; Wachs, I. E. The Influence of Metal Oxide Additives on the Molecular Structures of Surface Tungsten Oxide Species on Alumina: II. In Situ Conditions. *J. Mol. Catal. A: Chem.* **1998**, *132*, 59–71.
- (36) Wang, X.; Wachs, I. E. Designing the Activity/Selectivity of Surface Acidic, Basic and Redox Active Sites in the Supported K₂O–V₂O₅/Al₂O₃ Catalytic System. *Catal. Today* **2004**, *96*, 211–222.
- (37) Lewandowska, A. E.; Calatayud, M. n.; Lozano-Diz, E.; Minot, C.; Banares, M. A. Combining Theoretical Description with Experimental In Situ Studies on the Effect of Alkali Additives on the Structure and Reactivity of Vanadium Oxide Supported Catalysts. *Catal. Today* **2008**, *139*, 209–213.
- (38) Papp, S.; Korosi, L.; Meynen, V.; Cool, P.; Vansant, E. F.; Dekany, I. The Influence of Temperature on the Structural Behaviour of Sodium Tri- and Hexa-Titanates and Their Protonated Forms. *J. Solid State Chem.* **2005**, *178*, 1614–1619.
- (39) Mao, Y.; Wong, S. S. Size- and Shape-Dependent Transformation of Nanosized Titanate into Analogous Anatase Titania Nanostructures. *J. Am. Chem. Soc.* **2006**, *128*, 8217–8226.